

## Validity check of easy-to-use torsion test method for bioceramics

Kouichi Yasuda, Toshiyuki Kawano, Masanori Kikuchi, Mamoru Aizawa, Kanji Tsuru & Sadami Tsutsumi

To cite this article: Kouichi Yasuda, Toshiyuki Kawano, Masanori Kikuchi, Mamoru Aizawa, Kanji Tsuru & Sadami Tsutsumi (2018) Validity check of easy-to-use torsion test method for bioceramics, Journal of Asian Ceramic Societies, 6:1, 43-53, DOI: [10.1080/21870764.2018.1439613](https://doi.org/10.1080/21870764.2018.1439613)

To link to this article: <https://doi.org/10.1080/21870764.2018.1439613>



© 2018 The Author(s). Published by Informa UK Limited, trading as Taylor & Francis Group on behalf of The Korean Ceramic Society and The Ceramic Society of Japan



Published online: 26 Feb 2018.



Submit your article to this journal [↗](#)



Article views: 78



View related articles [↗](#)



View Crossmark data [↗](#)

## Validity check of easy-to-use torsion test method for bioceramics

Kouichi Yasuda<sup>a</sup>, Toshiyuki Kawano<sup>b</sup>, Masanori Kikuchi<sup>c</sup>, Mamoru Aizawa<sup>d</sup>, Kanji Tsuru<sup>e</sup> and Sadami Tsutsumi<sup>f</sup>

<sup>a</sup>Department of Materials Science and Engineering, Tokyo Institute of Technology, Tokyo, Japan; <sup>b</sup>Analytical and Measuring Instruments Division, Shimadzu Corporation, Kyoto, Japan; <sup>c</sup>Bioceramics Group, RCFM, National Institute for Materials Science, Tsukuba, Japan; <sup>d</sup>Department of Applied Chemistry, Meiji University, Tama-ku, Kawasaki-shi, Japan; <sup>e</sup>Section of Bioengineering, Department of Dental Engineering, Fukuoka Dental College, Fukuoka, Japan; <sup>f</sup>Tokyo Branch, Applied Electronics Laboratory, Kanazawa Institute of Technology, Tokyo, Japan

### ABSTRACT

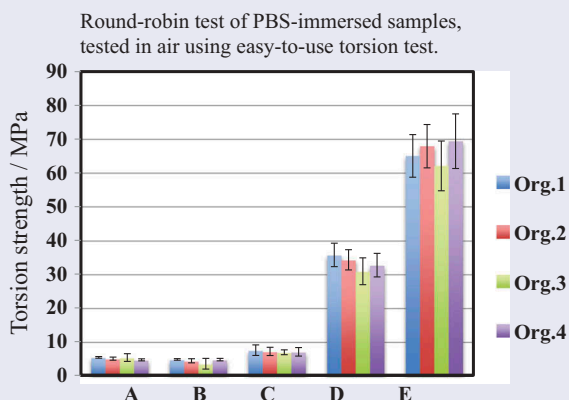
This article examines the validity of a test method to determine the torsion strength of bioceramics under *in-vivo*-mimicking circumstances. The torsion test setup consisted of upper and lower grip jigs, designed to grip dog bone-type bioceramic specimens, and an opening torque tester for PET bottles. A specimen was set on the torque tester through the lower grip jig at the bottom, and the upper grip jig was then mounted on the top end of the specimen. The upper grip jig was rotated by hand to apply torque until the specimen was fractured by the torsion. The torsion strength was calculated using the maximum torque at fracture and the gage diameter. Five calcium phosphate bioceramics were employed for the torsion test. The torsion strength data obtained by this method agreed closely with data measured using a material testing machine with a convertor from the linear crosshead motion into the rotation. Round-robin tests among four different organizations in Japan revealed that the torsion strength data showed good agreement for each sample immersed for 24 hr under phosphate-buffered solution as *in-vivo*-mimicking circumstances. These results verified the ability of the easy-to-use torsion method to give appropriate strength data with a simple experimental setup.

### ARTICLE HISTORY

Received 6 June 2017  
Accepted 22 December 2017

### KEYWORDS

Torsion test method; torsion strength; hydroxyapatite ceramics; validity check; bioceramics



## 1. Introduction

Bioceramics are regarded as key materials among advanced technologies because they play a role in many promising applications designed to improve people's quality of life in our aging society [1]. As society ages, the elderly will encounter problems such as bone fracture when they fall accidentally as well as gradual bone collapse resulting from osteoporosis (bone loss due to aging). To turn damaged human bones to an almost healthy condition, development of bioceramics is considered to be the task of pressing urgency [2].

In the past, dense  $\alpha$ - $\text{Al}_2\text{O}_3$  ceramics have been used for bone implantation and restoration, but it became apparent that the patients found it difficult to have  $\alpha$ - $\text{Al}_2\text{O}_3$  artificial bones replaced regularly (at about 10-year intervals). In order to avoid this problem, porous apatite ceramics have been developed, in which cells can penetrate into the pores and proliferate. And artificial bones (porous apatite ceramics) directly bind to natural bone at an early date [3–10]. This makes it clear that bioceramics must be strong enough not to be fractured or seriously damaged, even when subjected to abrupt loading during a clinical course. Until recently bending tests [5–7,10] have

been used to measure the strength of bioceramics, but torsion (or shear) tests have not been applied.

Torsion tests first appeared in the literature [11–13] in the 1950s in the engineering ceramics field. They later came to be used as a part of multiaxial fracture criterion studies, because the stress state  $\sigma_1 = -\sigma_2$  is pure torsion ( $\sigma_i$  stresses are principal stresses). The inclined-surface crack in flexure [14,15], biaxial tension by ball on ring [16], diametrical compression [17], and antisymmetrical bending [18] methods were also proposed for such the studies, but the tension/torsion test was considered the most fundamental test method. In 1981, Petrovic and Stout [19,20] reported tension/torsion tests of  $\alpha$ -Al<sub>2</sub>O<sub>3</sub> rod specimens, in which the principal stress ratio  $\sigma_2/\sigma_1$  was changed from 0 (pure tension) to  $-1$  (pure torsion) and found that the tensile fracture strength  $\sigma_{1f}$  increased with increases in the principal compressive stress  $\sigma_2$ . In their following articles [21,22], they also conducted axial tension, hoop tension, balanced biaxial tension, balanced tension-compression, and pure torsion tests for  $\alpha$ -Al<sub>2</sub>O<sub>3</sub> tube specimens. They reported, however that the balanced biaxial tensile strength was 10% lower than the uniaxial tensile strength, although no change was observed in the balanced tensile/compression strength, and also that the pure torsion strength was 16% higher than the uniaxial tensile strength. These controversial results were picked up again by Kim and Suh [23], who also investigated the tension/torsion behavior of  $\alpha$ -Al<sub>2</sub>O<sub>3</sub> tube specimens to consider the effect of minimum principal stress. Recently, torsion tests are also applied in the research on fatigue [24,25], PZT materials [26], and joining [27].

Conducting tension/torsion or pure torsion tests of bioceramics in the conventional way requires a material testing machine equipped with axial/rotational two-way grip chucks [28] (a system with a total cost as high as \$100,000). We must also prepare (1) dog bone-type specimens, (2) metal chuck sleeves, (3) a good setting alignment and strong bonding between the specimen and chuck sleeve, and (4) a multiple control system in which load and torque can

**Table 1.** Samples to be tested in torsion.

Sample	Material	Nominal porosity/%
A	Hydroxyapatite	75
B	Hydroxyapatite	75
C	Hydroxyapatite	50
D	Hydroxyapatite/tricalcium phosphate composites	35
E	Hydroxyapatite/tricalcium phosphate composites	0

be controlled simultaneously. Experts in mechanical testing can then conduct the tests, but the manufacturers and users of bioceramics cannot. As an alternative, we can purchase a more compact torsion tester [29] based on the lathe turning machine, but these are designed for torsion tests only. Since the cost will be several tens of thousands of dollars, it is not easy to prepare these machines, either.

With a view to the restricted conditions for torsion tests, the present authors have recently proposed an easy-to-use torsion test method for bioceramics [30]. This method requires only an opening torque tester for PET bottles [31] (costing approximately \$1,000) and simple grip jigs to enable anyone to conduct torsion tests anywhere with no special expensive setup. In a previous article [30], the present authors optimized this torsion test method by changing the specimen geometry and improving the jig mechanism to prevent bending moments and axial loading during torsion testing, and showed reasonable torsion strength data for blackboard chalk and five types of hydroxyapatite ceramics with different porosities.

In this article, we verify that the torsion strength data acquired by the easy-to-use torsion test method is accurate by comparing it with torsion strength data measured using a material testing machine equipped with a linear displacement/rotation convertor (using a rack-and-pinion gear system). For simplicity, the tests were done in air at ambient temperature. In the following, we confirm that good agreement can be seen in easy-to-use torsion strength data from four different organizations. In this test, the specimens

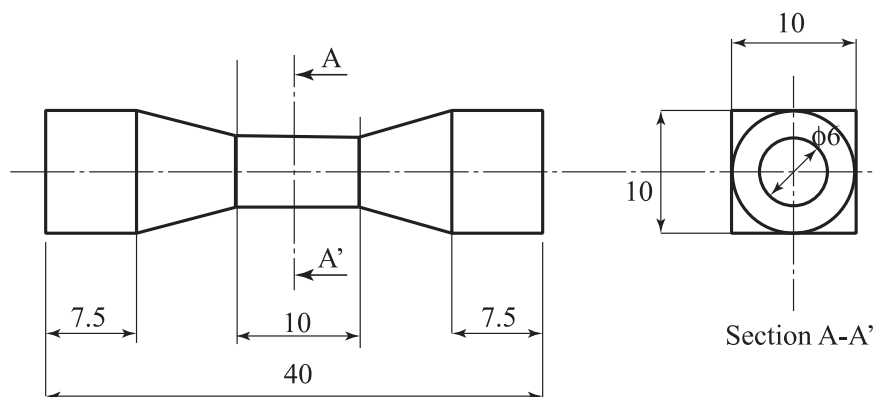


**Figure 1.** Specimen geometry.

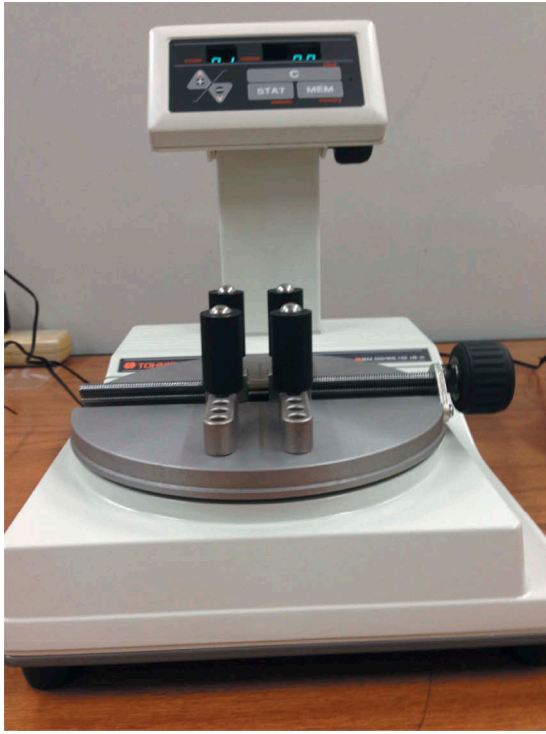


**Figure 2.** Opening torque tester for PET bottles.

were immersed in PBS (phosphate-buffered solution (PBS), which provides *in-vivo*-mimicking circumstances) for 24 hr at ambient temperature before torsion testing, because the final goal is to propose a torsion strength test method for PBS-immersed specimens as an ISO standard.

## 2. Experimental

### 2.1 Sample

Five types of bioceramics (denoted A, B, C, D, E, hereafter) were supplied by bioceramics companies in Japan. Precise information on their processing

and characterization was not open to us, except for the nominal porosity shown in Table 1. Samples A, B, and C were hydroxyapatite ceramics, and samples D and E were hydroxyapatite/tricalcium phosphate composites. These samples had been used in the previous study [30].

### 2.2 Specimen geometry

The specimen geometry was 40 mm in length, 10 mm in gage, and  $\phi 6$  mm in gage diameter, with tapering in a 2/7.5 slope, and prism ends as shown in Figure 1. Optimization of the specimen geometry was discussed in the previous article [30].

### 2.3 Easy-to-use torsion test

#### 2.3.1 Opening torque tester for PET bottles

Various torsion testers were available commercially. Most were developed as specialized machines for metallic automobile drive shafts [32], however, their torque capacity was also too large (e.g. maximum torque = 1000 Nm). We also considered more compact torsion testers [29]; their torque capacity was still large, however, at about 50 Nm. Thus, neither was directly applicable to bioceramics (typically 0.1 Nm or less for bioceramics in this study) due to large torque range and high cost of the testers.

Taking the future proposal for a “Test method for torsion strength of porous bioactive ceramics under *in-vivo*-mimicking circumstances” as an ISO standard for the future into account, the present authors decided to assemble a torsion test system that is as simple as possible to enable anyone to conduct tests anywhere without expensive specialized equipment. To satisfy these conditions, we focused on an opening torque tester for PET bottles incorporating simple grip jigs.



**Figure 3.** Grip jigs (the left is upper grip jig, and right is lower grip jig attached with a plastic sleeve guide).

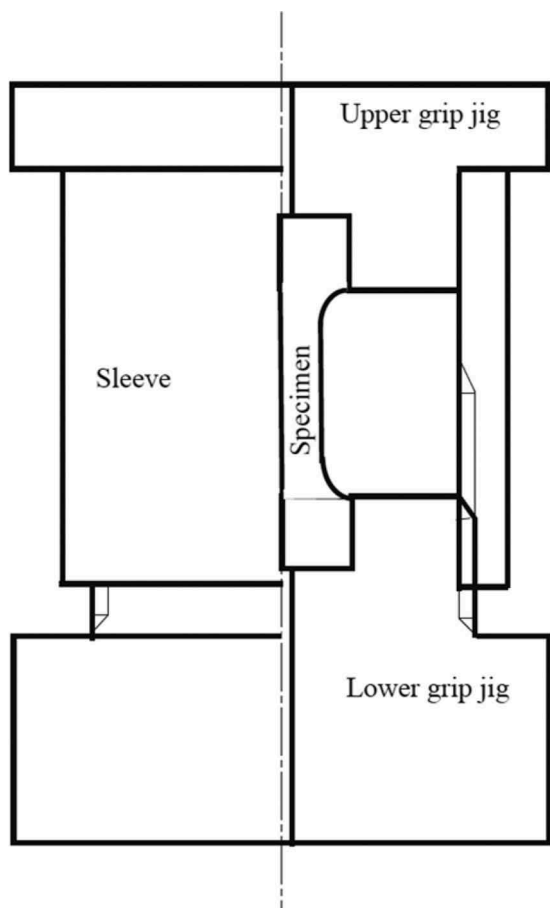


**Figure 4.** Semi-sectioned drawing of grip jigs (the left half is outlook, right half is sectioned).

Figure 2 shows an opening torque tester for PET bottles (Tohnichi Mfg. Co. Ltd: 2TME500CN2) [31]. This tester was used for checking the opening torque of PET bottles within a designated range using the following test procedure: to hold PET bottle, four rubber-covered pillars were moved radially toward the center of the round-based table by rotating a black nob on the right side; the PET bottle cap was rotated by hand; and the maximum opening torque was displayed in a window at the top. Thus, this tester already had three functions: holding the object, measuring the torque (a torque cell was installed below the round-based table), and displaying the maximum torque upon opening. We therefore prepared only simple specimen grip jigs to

conduct torsion tests for bioceramics. Actually, the present authors used two types of testers (Tohnichi Mfg. Co. Ltd: 2TME500CN2 (100–500 cNm) and 2TME200CN2 (40–200 cNm)) depending on the torque range applied. Several companies around the world make similar opening torque testers for PET bottles.

### 2.3.2 Grip jigs with sleeve guide

As shown in Figure 3, the grip jigs were two-stepped circular cylinders with a square hole in the center of the smaller base planes. The smaller circular cylindrical part of the upper (left) grip jig had a smooth outer surface that fit the smooth inner side surface of the plastic sleeve guide to fix the rotation axis when the upper grip jig was rotated by hand. The smaller circular cylindrical part of the lower (right) grip jig had a long threaded outer side surface whose tread fit the inner thread of the plastic sleeve guide in order to adjust the height of the guide when rotated along the tread. This sleeve guide had two functions: to prevent bending moments and to cancel axial load during torsion tests. The inner structure is shown in Figure 4 (semi-sectioned drawing). To avoid blank test calibrations, the upper grip jig was made of aluminum alloy (not a heavy metal).

### 2.3.3 Easy-to-use torsion test

A lower grip jig was attached to an opening torque tester for PET bottles, and one end of the specimen was inserted into a square hole in the grip jig (Figure 5(a)). The other end of specimen was also inserted into the upper grip jig (Figure 5(b)). The plastic sleeve guide was moved upward by its rotation. When its top end touched the upper grip jig, the sleeve guide was moved up slightly to cancel the weight of the upper grip jig (Figure 5(c)). The upper grip jig was then rotated by hand to apply torque until the specimen was fractured by the torsion (Figure 5(d)). The time to fracture was within 1–2 s, and it was thus considered that slow crack growth had little effect on the torsion strength values.

A blank test should be conducted before the torsion tests by rotating the upper grip jig without a specimen. When the upper grip jig was made of aluminum alloy, the blank test value was almost 0.0 cNm; however, the

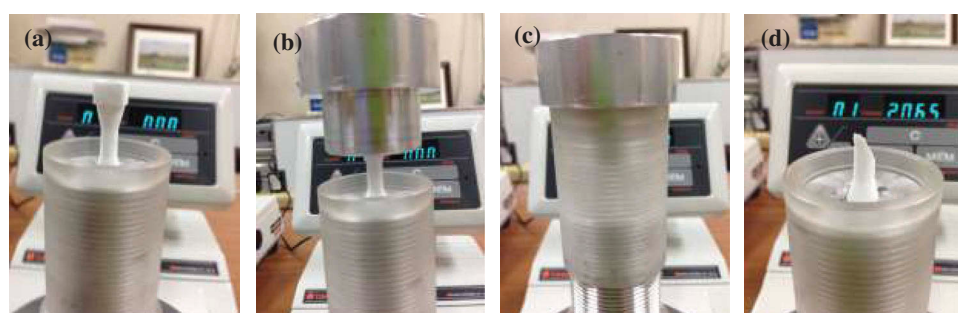


**Figure 5.** Easy-to-use torsion test using the grip jigs.

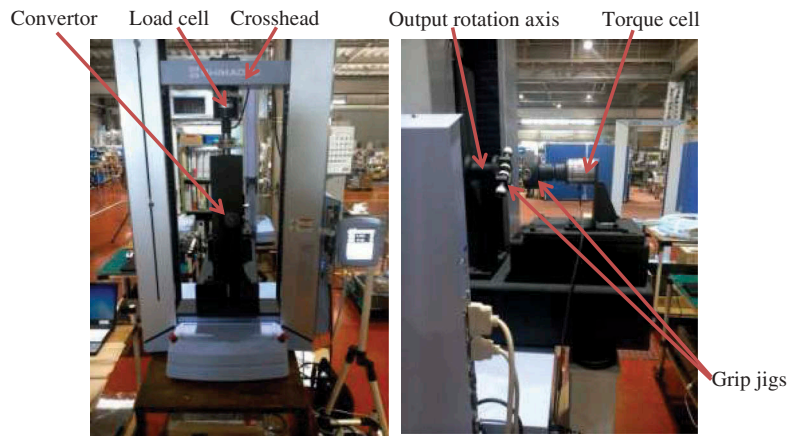
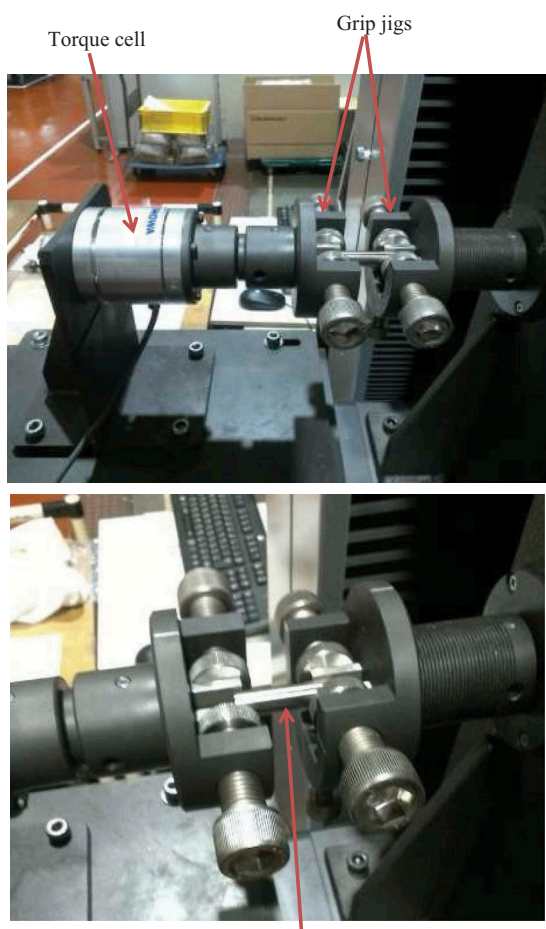


**Figure 6.** A material testing machine (Shimadzu, Autograph AG-X) equipped with a linear displacement/rotation convertor (Shimadzu, STJ-10, using a rack-and-pinion gear system).



Alignment check by cylindrical metal dummy specimen

**Figure 7.** Expanded view of grip jig and alignment check using a cylindrical dummy specimen.

value was around 2–3 cNm when we used stainless steel due to the friction between the top end of the sleeve guide and the upper grip jig. In this study, the present authors used an aluminum alloy upper grip jig (no need for calibration). If the blank test value is 2–3 cNm when using a stainless-steel upper jig, the blank test value must be subtracted from each torque measurement at fracture for calibration.

#### **2.4. Torsion test with a material testing machine equipped with a linear displacement/rotation convertor**

To investigate the accuracy of the easy-to-use torsion test data, a material testing machine (Shimadzu, Autograph AG-X) was used to measure the torsion strength of the same samples. The material testing machine was equipped with a linear displacement/rotation convertor (Shimadzu, STJ-10). As shown in Figure 6, the convertor had a rack-and-pinion gear system to transform the linear displacement of the crosshead movement into rotation of the output axis toward the backside of the testing machine. One grip jig (right jig in Figure 7) was attached to this output axis, and another grip jig (left jig in Figure 7) was attached to the torque cell. The torque cell (10 Nm max. capacity, 0.01 Nm(=1 cNm) min. accuracy) was fixed to the rigid frame of the testing machine. The rotation test speed was set at 50 °/min by adjusting the crosshead speed of the material testing machine such that the time to fracture was within 3–4 s in this case as well.

As shown in Figure 7 (lower figure), a dummy specimen was set between the two flat metal plates of the grip jig. The centering of the interval between the plates with respect to the output rotation axis can be adjusted by rotating each hexagonal bolt separately. Note that the interval of the two plates was lightly fitted to the grip end of the specimen, rather than firmly fixed, so that the axial displacement of the specimen was free during the torsion test. We used the dummy specimen to adjust the alignment between the rotation axis and the two grip jigs.

In this verification, torsion testing with a material testing machine equipped with a convertor was conducted in air by the organization ID = 5 and the number of specimen was 5. The easy-to-use torsion tests, on the other hand, were conducted in air by the organization ID = 1, and the number of specimen was 10 for each sample. Torsion data from both tests were compared.

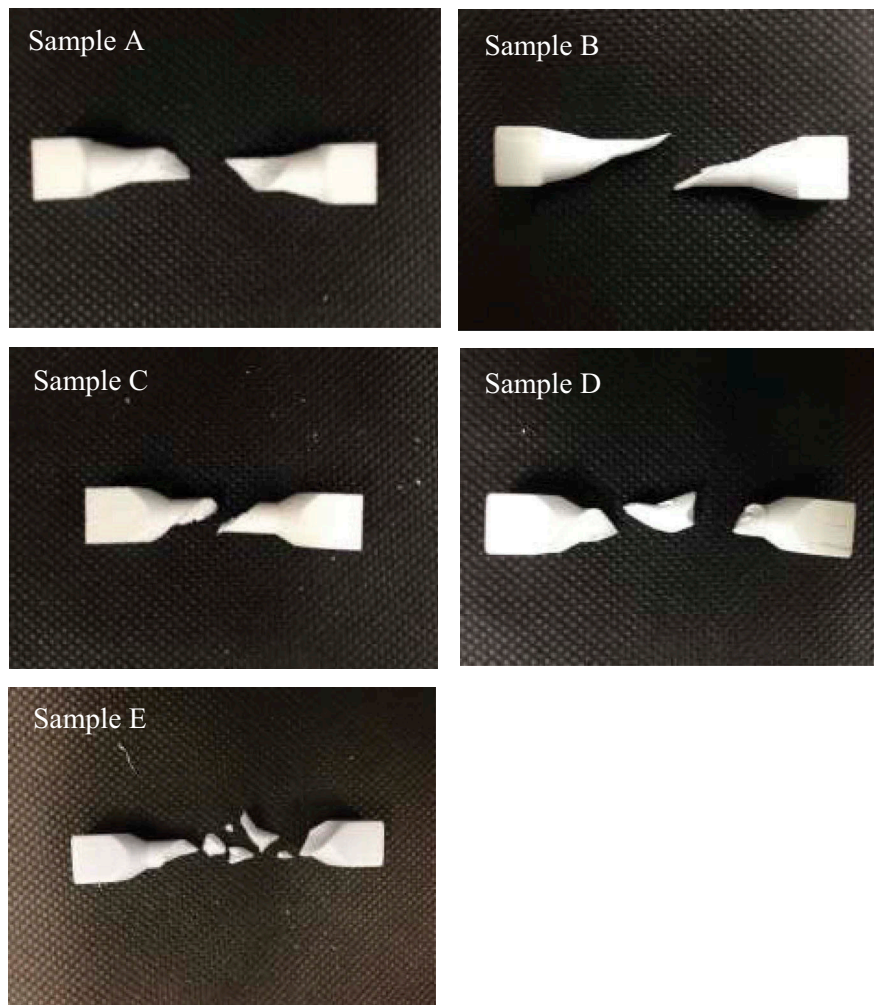


**Figure 8.** Fracture surfaces of as-received samples tested in air using the easy-to-use torsion test method (by organization 1).

**Table 2.** Torsion strength in air using easy-to-use torsion test (as-received specimen, measured by organization 1).

Sample	Material (Nominal porosity)	Average torsion strength/ MPa	Standard deviation of torsion strength/ MPa
A	Hydroxyapatite (75%)	5.21	0.61
B	Hydroxyapatite (75%)	4.85	0.40
C	Hydroxyapatite (50%)	8.21	1.30
D	Hydroxyapatite/tricalcium phosphate composites (35%)	35.1	4.14
E	Hydroxyapatite/tricalcium phosphate composites (0%)	86.9	3.41

## 2.5 Round-robin test

Four organizations (ID = 1–4) in Japan participated in this round-robin test in order to confirm good agreement in torsion strength data when different people conducted the easy-to-use torsion test. Prior to this set of torsion tests, all the specimens were immersed in PBS (pH = 7.4) for 24 hr at ambient temperature. During immersion, the specimens

were evacuated once for 30 min or longer to eliminate air in the pores to the extent. Then, just before each torsion test, a specimen was picked out, and the wet surface was wiped with paper. The easy-to-use torsion tests were conducted according to the procedure in Section 2.3. The number of specimen was 10 for each sample, except in the case of the organization ID = 3. Organization ID = 3 tested five as-received specimens in air and five specimens tested in air after immersion in PBS.

## 3. Results and discussion

### 3.1 Accuracy check

#### 3.1.1 Easy-to-use torsion test in air

Easy-to-use torsion tests of as-received specimens in air were conducted by organization ID = 1, and their fracture surfaces are shown in Figure 8. From this figure, it can be seen that samples A, B, and C showed helical fracture surfaces, which are a typical feature of torsion fracture of brittle materials. According to the mechanics of materials [33], a pure torsion stress state is equivalent to a

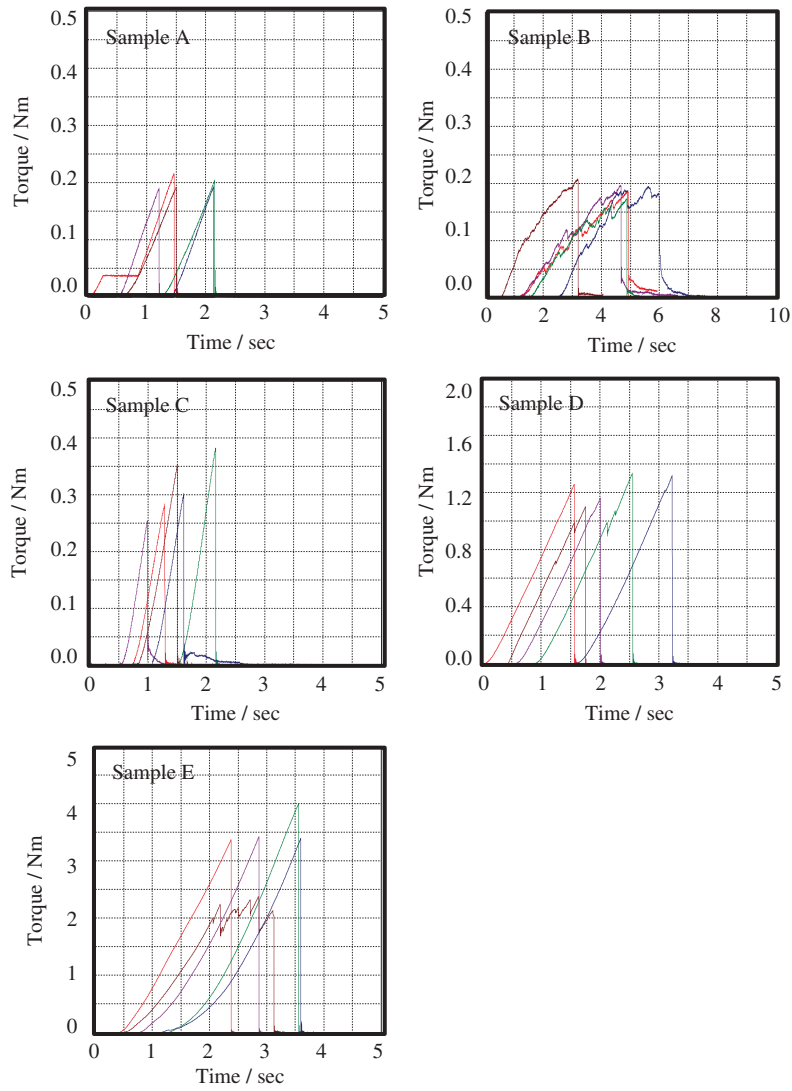


**Figure 9.** Torque/time ( $\propto$  rotation angle) diagrams of as-received samples.

**Table 3.** Torsion strength in air using a material testing machine (as-received specimen, measured by organization 5).

Sample	Material (Nominal porosity)	Average torsion strength/ MPa	Standard deviation of torsion strength/ MPa
A	Hydroxyapatite (75%)	4.72	0.26
B	Hydroxyapatite (75%)	4.53	0.29
C	Hydroxyapatite (50%)	7.43	1.20
D	Hydroxyapatite/tricalcium phosphate composites (35%)	29.0	2.45
E	Hydroxyapatite/tricalcium phosphate composites (0%)	77.9	13.5

tensile/compression biaxial stress state achieved by  $45^\circ$  rotation of the original  $x$ - $y$  coordinate system. Thus a crack extended along the normal direction to the tensile stress (viz. the crack always extended with an incline of  $45^\circ$  to the longitudinal axis of the specimen). On the contrary, samples D and E

show multiple fractures (fragmentation occurred during fracture), but if we look at them more closely, we find a partial helical fracture surface. Samples D and E show relatively higher torsion strength due to lower porosity and such multiple fractures can also be seen after bending tests of high-strength dense ceramics.

By measuring the maximum torque at fracture  $T_f$  of each specimen, we calculated the torsion strength  $\tau_f$  using the following equation [34];

$$\tau_f = \frac{16T_f}{\pi d^3} \quad (1)$$

where  $d$  is the gage diameter ( $\phi 6$  mm in this study). The average and standard deviation of torsion strength are summarized in Table 2. The torsion strength increased with decreases in the porosity, and the standard deviation was around 1/10 of its average, indicating that the data for the easy-to-use torsion test method showed good accuracy (no large data scattering).

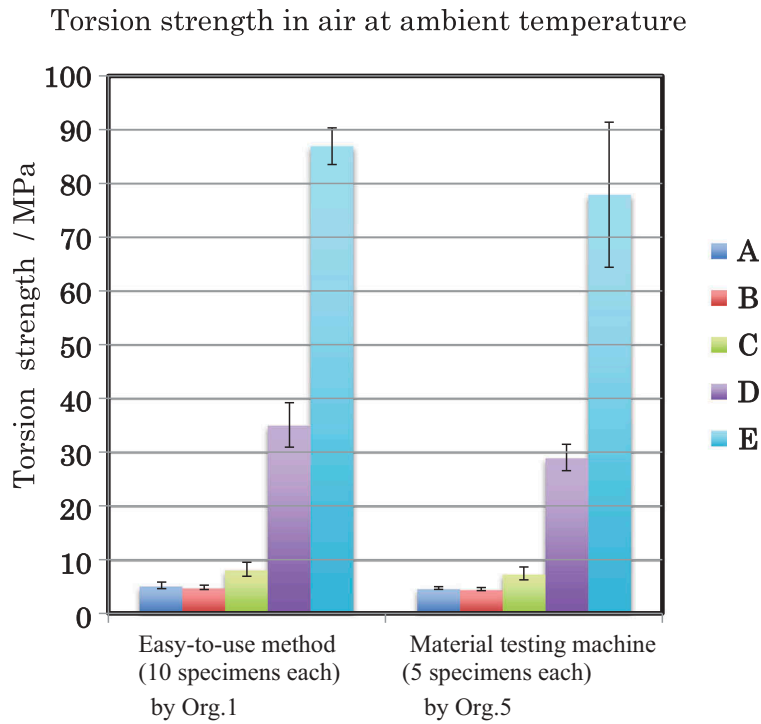


**Figure 10.** Comparative study of easy-to-use method and a material testing machine with a convertor (as-received specimens in air).

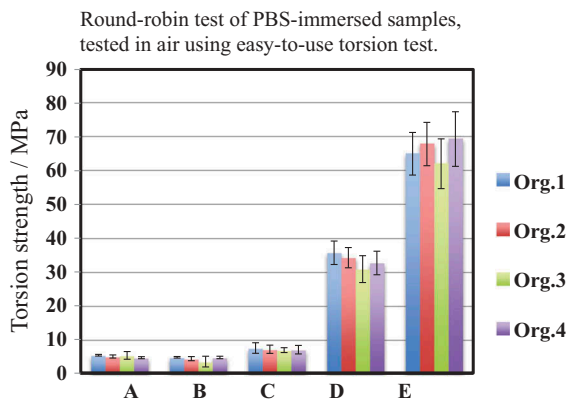


**Figure 11.** Round-robin test of torsion strengths of samples after PBS immersion for 24 hr, tested in air using easy-to-use torsion tests (by organization 1, 2, 3, 4).

### 3.1.2 Torsion test in air conducted with a material testing machine equipped with a convertor

Torsion tests of as-received specimens were conducted in air by organization ID = 5 using a material testing machine equipped with a convertor, and the resulting fracture surfaces were the same as those in Figure 8. Figure 9 shows their torque/time ( $\propto$ rotation angle) diagrams. Most of the samples except B showed linear elastic deformation and then brittle fracture. In sample B, linear elastic deformation was observed, followed by nonlinear deformation and then brittle fracture. We used the maximum torque as the torque at fracture in our calculations. As stated earlier, the time to fracture  $t_f$  was around 3–4 s, so the rotation angle  $\phi_f$  at fracture was around  $5.8 \times 10^{-2}$  [rad]

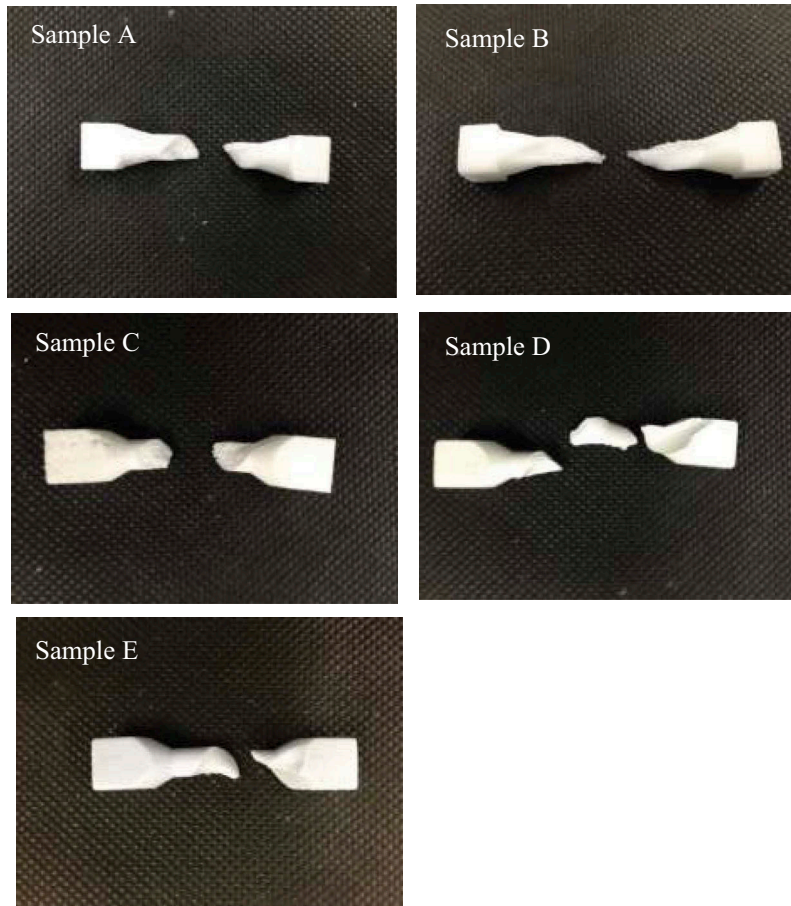
( $= t_f[\text{sec}] \times 50[^\circ/\text{min}] \times (\pi[\text{rad}]/180[^\circ])/60[\text{sec}]$ ) ( $= 4 \times 50 \times (\pi/180)/60$ ), and the shear strain at fracture was therefore  $\gamma_f = r \times \phi_f/L = (3 \times 10^{-3}) \times (5.8 \times 10^{-2})/(10 \times 10^{-3}) = 1.7 \times 10^{-2}$ , where  $L$  and  $r$  were the gage and its radius.

Table 3 shows the average and standard deviation of torsion strength measured by the material testing machine with the convertor, and Figure 10 shows a comparison between the data obtained by the easy-to-use torsion method (in Table 2) and the material testing machine method (Table 3). At a glance, we can see that almost the same results were obtained by the two measurement methods.

In the comparison, all the samples show good agreement in average torsion strength measurement results for the easy-to-use method and the material testing machine method, indicating that the easy-to-use torsion test method gives data with good accuracy data, comparable to data obtained by the material testing machine.

### 3.2 Round-robin test

Four organizations (ID = 1, 2, 3, 4) conducted torsion tests of specimens immersed in PBS (pH = 7.4) for 24 hr at ambient temperature. A comparison of the results obtained by the 4 organizations is shown in Figure 11. Note that organization ID = 3 tested 5 specimens and the others tested 10 specimens for each sample. At first glance, we see good agreement in the average torsion strength for each sample among the four organizations, indicating an absence of experimenter effect.



**Figure 12.** Fracture surfaces of samples after PBS immersion for 24 hr, tested in air using easy-to-use torsion tests (by organization 1).

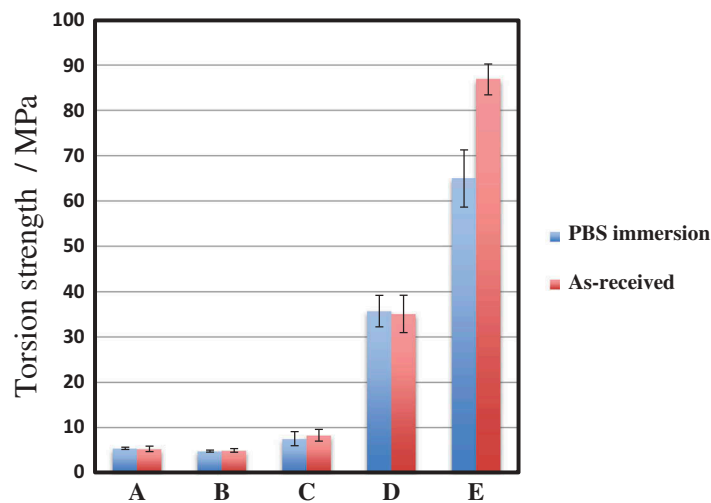


**Figure 13.** Torsion strength of as-received samples (■) and samples (■) after PBS immersion for 24 hr, tested in air using easy-to-use torsion tests (by organization 1).

Within the experimental data in this study, the easy-to-use torsion test method is useful for obtaining reasonable torsion strength data, which is in good agreement among different organizations and which clearly shows the differences in the samples.

### 3.3 Comparison between as-received samples and PBS-immersed samples

Organization ID = 1 conducted torsion tests for both as-received samples (Table 2) and PBS-immersed samples (Figure 11). Thus we can compare the as-received samples and PBS-immersed samples. Figure 12 shows the

fracture surfaces of the samples after PBS immersion for 24 hr, and testing in air by the easy-to-use torsion method. Comparing these with Figure 8, we see that samples A, B, C, and D show the same fracture features as the as-received samples, but that sample E shows a typical helical fracture surface, not multiple fracture as in Figure 8. This corresponds to the tendency shown in Figure 13, which is a comparison between the torsion strengths of as-received samples and PBS-immersed samples. Only sample E shows a difference between the two data, which may have been brought about by slow crack growth during PBS immersion.

In the torsion tests, the maximum stress was formed at the cylindrical surface of the gage, and in dense sample E, the weakest defect (largest defect) on the surface was relatively smaller than that in other samples, and slow crack growth during PBS immersion consequently had a significant effect on its crack extension. Since samples A, B, C, and D were porous, the original weakest defect was relatively larger in size; so crack extension by slow crack growth did not have much effect on the final crack size (weakest defect size). These data suggest that not only as-received samples but also PBS-immersed samples are important for estimating the reliability of bioceramics.

#### 4. Conclusion

The easy-to-use torsion test method was verified by two experiments. One was an accuracy check comparing torsion strength data measured by the easy-to-use method with data obtained using a material testing machine equipped with a linear displacement/rotation convertor. Good agreement was shown between the results for the two methods. The other was a round-robin test conducted by four different organizations in Japan, which found that the torsion strength data did not depend on the organization, and that consistent test data were obtained. Based on these experimental results, it is concluded that the easy-to-use torsion method gives reasonable strength data with a simple experimental setup, and that it can be proposed as ISO standard for the future.

#### Acknowledgments

This research was supported in part by the Ministry of Economy, Trade and Industry, Japan as a project undertaken for International Standardization for test method for torsion strength of porous bioactive ceramics under *in-vivo*-mimicking circumstances. The authors wish to express our gratitude to Mr. Tsutomu ARAI (Tohnichi Mfg. Co. Ltd.) for his technical advice on torque measurements, to bioceramics manufacturers for supplying samples, and to the Japan Fine Ceramics Association for its invaluable administrative support.

#### Disclosure statement

No potential conflict of interest was reported by the authors.

#### ORCID

Kouichi Yasuda  <http://orcid.org/0000-0002-2681-7516>

#### References

- [1] The WHOQOL Group. The World Health Organization quality of life assessment (WHOQOL): position paper from the World Health Organization. *Soc Sci Med.* 1995;41:1403–1409.
- [2] Tsutsumi S. Trend report on international and Japanese standardization activities for bioceramics and tissue engineered medical products. *Sci Technol Adv Mater.* 2010;11(3):014112.
- [3] Aoki H, Kato K. Apatites as biomaterials. *Ceramics.* 1975;10: 469–478. in Japanese.
- [4] Jarcho M, Bolen CH, Thomas MB, et al. “Hydroxylapatite synthesis and characterization in dense polycrystalline form”. *J Mater Sci.* 1976;11:2027–2035.
- [5] Metsger DS, Rieger MR, Foreman DW. Mechanical properties of sintered hydroxyapatite and tricalcium phosphate ceramic. *J Mater Sci Med.* 1999;10:9–17.
- [6] Zyman ZZ, Ivanov IG, Glushko VI. “Possibilities for strengthening hydroxyapatite ceramics”. *J Bio Med Mater Res.* 1999;46:73–79.
- [7] Kawata M, Uchida H, Itatani K, et al. Development of porous ceramics with well-controlled porosities and pore sizes from apatite fibers and their evaluations. *J Mater Sci: Mater Med.* 2004;15:817–823.
- [8] Kikuchi M, Ikoma T, Syoji D, et al. Porous body preparation of hydroxyapatite/collagen nanocomposites for bone tissue regeneration. *Key Eng Mater.* 2004;254–256:561–564.
- [9] Ishikawa K, Koga N, Tsuru K, et al. Fabrication of interconnected porous calcite by bridging calcite granules with dicalcium phosphate dihydrate and their histological evaluation. *J Biomed Mater Res A.* 2016;104(3):652–658.
- [10] Shiota T, Shibata M, Yasuda K, et al. “Influence of  $\beta$ -tricalcium phosphate dispersion on mechanical properties of hydroxyapatite ceramics”. *J Ceram Soc Jpn.* 2008;116:1002–1005.
- [11] Salmassy OK, Duckworth WH, Schwoppe AD. Behavior of brittle-state materials. WADC Tech. Rep. No.53-50, Part I. Battelle Memorial Institute; June 1955.
- [12] Cameron NM. The phenomenon of fracture morphology of glass tested in tension, flexure and torsion. Department of Theoretical and applied Mechanics, University of Illinois. T & A M Rep; 1963 Apr; 242, AD 402795.
- [13] Priddle EK. Effect of multiaxial stresses on the fracture strength of silicon carbide. *J Strain Anal.* 1969;4:81–87.
- [14] Petrovic JJ, Mendiratta MG. Mixed-mode fracture from controlled surface flaws in hot-pressed  $\text{Si}_3\text{N}_4$ . *J Am Ceram Soc.* 1976;59(3–4):163–167.
- [15] Petrovic JJ. Mixed-mode fracture of hot-pressed  $\text{Si}_3\text{N}_4$ . *J Am Ceram Soc.* 1985;68(6):348–355.
- [16] Shetty DK, Rosenfield AR, Bansal GK, et al. Biaxial fracture studies of a glass-ceramic. *J Am Ceram Soc.* 1981;64(1):1–4.

- [17] Shetty DK, Rosenfield AR, Duckworth WH. Mixed-mode fracture of ceramics in diametral compression. *J Am Ceram Soc.* 1986;69(6):437–443.
- [18] Suresh S, Shih CF, Morrone A, et al. Mixed-mode fracture toughness of ceramic materials. *J Am Ceram Soc.* 1990;73(6):1257–1267.
- [19] Petrovic JJ, Stout MG. Fracture of  $\text{Al}_2\text{O}_3$  in combined tension/torsion: I, experimentals. *J Am Ceram Soc.* 1981;64(11):656–660.
- [20] Petrovic JJ, Stout MG. Fracture of  $\text{Al}_2\text{O}_3$  in combined tension/torsion: II, weibull theory. *J Am Ceram Soc.* 1981;64(11):661–666.
- [21] Stout MG, Petrovic JJ. Multiaxial loading fracture of  $\text{Al}_2\text{O}_3$  tubes: I, experiments. *J Am Ceram Soc.* 1984;67(1):14–18.
- [22] Petrovic JJ, Stout MG. Multiaxial loading fracture of  $\text{Al}_2\text{O}_3$  tubes: II, weibull theory and analysis. *J Am Ceram Soc.* 1984;67(1):18–23.
- [23] Kim KT, Suh J. Fracture of alumina tubes under combined tension/torsion. *J Am Ceram Soc.* 1992;75(4):896–902.
- [24] Suresh S, Tschegg EK. Combined mode-I-mode III fracture of fatigue-precracked alumina. *J Am Ceram Soc.* 1987;70(10):726–733.
- [25] Schwind T, Kerscher EK, Lang K-H. Fatigue of alumina under cyclic torsion loading. *Adv Eng Mater.* 2009;11(7):586–589.
- [26] Fett T, Munz D, Thun G. Multiaxial deformation behavior of PZT from torsion tests. *J Am Ceram Soc.* 2003;86(8):1427–1429.
- [27] Ferraris M, Salvo M, Casalegno V, et al. Torsion tests on AV119 epoxy – joined SiC. *Int J Appl Ceram Technol.* 2012;9[4]:795–807.
- [28] For example, Shimadzu, Axial force and torsion testing machine [Internet]. [cited 2017 Jun 6]. Available from: <http://www.shimadzu.com/an/test/fatigue/axial-torsion.html>
- [29] For example, Instron, MT Series Low Capacity Torsion Testers [Internet]. [cited 2017 Jun 6]. Available from: <http://www.instron.us/en-us/products/testing-systems/torsion-systems/low-capacity?region=North%20America&lang=en-US>
- [30] Yasuda K, Tsutsumi S. Challenges in development of easy-to-use torsion test method for bioceramics - toward ISO standard proposal. The Proceedings of the 41st International Conference on Advanced Ceramics and Composites (American Ceramic Society, Jan 22-27, 2017, Daytona Beach, FL, USA): Ceramic Engineering and Science Proceedings, Volume 38, Issue 2 (eds J. Salem, J. C. LaSalvia, R. Narayan, D. Zhu), John Wiley & Sons, Inc., Hoboken, NJ, USA. 2018.
- [31] For Example, Tohnichi, Torque Meter [Internet]. [cited 2017 Jun 6]. Available from: <https://en.global-tohnichi.com/products/categories/32>
- [32] For Example, Tinius Olsen Testing Machine Company, Torsion Tester [Internet]. [cited 2017 Jun 6]. Available from: <https://www.tiniusolsen.com/list-of-products/torsion-testers>
- [33] Gere JM, Timoshenko SP. Mechanics of materials. 3rd ed. Chapter 3, Torsion. Boston: PWS Publishing Company; 1990. p. 173.
- [34] Timoshenko SP, Goodier JN. The theory of elasticity. Torsion: MacGrow-Hill Book Company;1951 264. Chapter 11.